RSC Advances

PAPER

View Article Online
View Journal | View Issue

Cite this: *RSC Adv.*, 2020, **10**, 19803

Green synthesis and characterisation of novel [1,3,4]thiadiazolo/benzo[4,5]thiazolo[3,2-*a*] pyrimidines *via* multicomponent reaction using vanadium oxide loaded on fluorapatite as a robust and sustainable catalyst†

Nagaraju Kerru, Lalitha Gummidi, Surya Narayana Maddila, Sandeep V. H. S. Bhaskaruni, Suresh Maddila and Sreekantha B. Jonnalagadda *

Received 11th March 2020
Accepted 19th May 2020

DOI: 10.1039/d0ra02298e

rsc.li/rsc-advances

We synthesised materials with different loadings of vanadia on fluorapatite (V_2O_5/FAp), fully characterised their structural properties using various spectral techniques including TEM, BET, XRD, FT-IR, SEM and EDX and assessed their prowess as catalysts. The 2.5% V_2O_5/FAp exhibited excellent activity for the synthesis of novel [1,3,4]thiadiazolo[3,2-*a*]pyrimidines and benzo[4,5]thiazolo[3,2-*a*]pyrimidines. The one-pot three-component fusion reaction between chosen substrates of 1,3,4-thiadiazole-amines or 2-amino-benzothiazole, aldehydes and active methylene compounds in ethanol solvent at room temperature gave an excellent yield of products (90–97%) in a swift reaction (25–30 min). The advantages of this protocol are rapid synthesis, mild reaction conditions, green solvent, easy work-up, eco-friendliness, reusability of catalyst and no need for column chromatography.

Introduction

In organic synthesis, the use of green principles and efficient catalysts to achieve excellent yields is always a cherished goal.[1] In recent times, the use of heterogeneous catalysts in organic synthesis has significantly increased, due to their stability and tunable properties.[2] Fluorapatite (FAp) ($Ca_{10}(PO_4)_6F_2$) is an inexpensive material with the capability to accommodate different anionic and cationic ions, making it suitable for several applications.[3] FAp crystallises in a hexagonal crystal arrangement, with phosphate and calcium ions arranged over the fluoride ions.[4] Due to its remarkable ion exchangeability with a variety of metal ions, it is a component of different frame supported metal composites, with high stability and tunable acid–base properties.[4] The tunable properties of FAp and metal amended FAp have imparted flexibility as heterogeneous catalysts. The multiple active sites (Lewis/Brønsted acidic and basic sites), present could facilitate different valuable organic conversions.[5] The acidic sites are produced from the PO_4 group of phosphorous and Ca^{2+}. The basic sites are generated from the PO_4 group of oxygen and F^-, which are tightly crammed on its fluorapatite surface.[6] Several fluorapatite has been explored as catalysts for the carbon–carbon and carbon–nitrogen bond construction reactions.[7–9] FAps also play an essential role in numerous biomedical applications.[10] Thus, FAp proves an ideal material for a broad spectrum of applications, including catalysis. Likewise, supported metal oxide catalysts have been utilised over the years in various synthetic organic applications.[11] Many transition metal oxides, in particular, vanadium oxide are known as efficient heterogeneous catalysts in several value-added organic transformations.[12–14] The empty d-orbitals of vanadium cation serve as electron acceptor sites, and oxyanions serve as electron donors rendering good surface catalytic properties to vanadia.[15,16] The acid–base pairs of vanadium oxides also increase their importance in catalytic science. Recently, our research group reported the synthesis and characterization of various metal loaded fluorapatite materials and their scope as heterogeneous catalysts in multicomponent organic synthesis with excellent yields.[17–20] Based on that experience, we examined the synergic activity of fluorapatite and vanadium oxide to enhance the efficiency of value-added organic conversions.

Multicomponent reaction (MCR) is a valued technique in organic synthesis, drug innovation platforms and the development of a range of biologically relevant molecules. Broadly used MCR, of Biginelli type, involves the cyclo-condensation of an aldehyde, active methylene compounds and various aminoazoles, to give the corresponding dihydropyrimidines.[21,22] MCR heterocyclisations involving aminoazoles are key building blocks in synthesis, as they especially contain alternative

School of Chemistry & Physics, University of KwaZulu-Natal, Westville Campus, Chiltern Hills, Durban-4000, South Africa. E-mail: jonnalagaddas@ukzn.ac.za; Fax: +27 31 2603091; Tel: +27 31 2607325

† Electronic supplementary information (ESI) available. See DOI: 10.1039/d0ra02298e

nucleophilic reaction centres facilitating their cyclo-condensations with carbonyl and active methylene compounds.[23–26] The MCR approach in organic synthesis, in combination with green solvents and recyclable catalysts, has created a cost-effective and ecologically positive impact on the chemical and pharmaceutical arenas.

The chemistry of the fused heterocycles, 1,3,4-thiadiazole-pyrimidines and benzo[4,5]thiazolo[3,2-*a*]pyrimidines is of continued interest. These are well-known structural analogues of various building blocks in several drug candidates.[27] The synthesis of novel functionalized [1,3,4]thiadiazolo[3,2-*a*] pyrimidine and benzo[4,5]thiazolo[3,2-*a*]pyrimidines received significant attention from the synthetic and medicinal chemists, owing to their wide variety of biological profiles, including the antitubercular and antibacterial,[28] antiviral,[29,30] anti-cancer,[31] antibiofilm[32] and antitumor[33] activities. Therefore, the syntheses of 1,3,4-thiadiazole/benzothiazole-pyrimidine derivatives are highly valuable for their immense pharmacological potential.

However, many synthetic protocols are not straightforward and involve multiple steps, often demanding the separation and purification of the reaction intermediates. For example, 2-sulfamoyl-5*H*-[1,3,4]-thiadiazolo[3,2-*a*]pyrimidine-6-carboxamides were synthesised from 5-amino-[1,3,4]thiadiazole-2-sulfonamide *via* a two-step approach.[34] Azab *et al.* have reported a two-step method for 5*H*-1,3,4-thiadiazolo[3,2-*a*] pyrimidin-5-ones, which involved the reaction of 2-amino-1,3,4-thiadiazoles to ethyl cyanoacetate and tandem reduction and deamination in the presence of phosphorus pentoxide–formic acid.[35] Zhao *et al.* have described the synthesis of 5*H*-[1,3,4]thiadiazolo[3,2-*a*]pyrimidine-6-carboxylate derivatives using aldehydes, 2-amino-thiadiazole and acetoacetate by one-pot MCR strategy under microwave irradiation.[36] The synthesis of anticancer compounds, 7-substituted-phenyl-8,8a-dihydro-7*H*-[1,3,4]thiadiazolo[3,2-*α*]pyrimidine-6-carbonitriles was achieved by Tiwari and co-workers from the one-pot reaction of 5-(4-chlorophenyl)-1,3,4-thiadiazol-2 amine, aromatic aldehydes and malononitrile under ultrasonic irradiation and NaOH.[37] Recently, Kasaboina *et al.* have also reported the synthesis of benzosuberone-linked to thiadiazolo[3,2-*a*] pyrimidine-6-carboxylates reacting benzosuberone with 1,3,4-thiadiazol-2 amine, ethyl acetoacetate and substituted benzaldehydes in polyethylene glycol (PEG) under reflux condition.[38] Recent literature also shows the increased interest of researchers towards the synthetic protocols for benzothiazole-pyrimidine derivatives. Many types of catalysts have been described to promote the synthesis of benzothiazole-pyrimidine derivatives *via* a three-component reaction of aldehydes, 2-aminobenzothiazole and *β*-keto ester. The different heterogeneous catalysts employed include Fe_3O_4@nano-cellulose/Cu(II), nano-kaolin/Ti^{4+}/Fe_3O_4, nano-cellulose/BF_3/Fe_3O_4 and nano-Fe_3O_4@SiO_2–$TiCl_3$, to mention a few.[26,39–41]

Although [1,3,4]thiadiazole-pyrimidine synthetic procedures involving MCRs exist, many suffer from the by-product formation, lesser yields and need for hazardous chemicals or harsh reaction conditions. Thus, from the viewpoint of environmental safety and sustainability, it is rewarding to design efficient green one-pot methodologies to synthesise the 1,3,4-thiadiazole/benzothiazole-pyrimidine analogues, which can provide better yields in shorter reaction times and substrates variability.

In our endeavour to develop new and green methodologies by exploring MCR strategy, we earlier reported a few value-added organic conversion protocols involving reusable heterogeneous catalysts for libraries of different biological potent heterocycles.[18–20] Based on the literature survey, no studies are available using a combination of vanadium oxide loaded fluorapatite as catalyst in synthetic organic applications. This communication describes the preparation of materials with different wt% vanadia loaded on fluorapatite, and a simple one-pot procedure for the synthesis of novel [1,3,4]thiadiazolo[3,2-*a*] pyrimidine and benzo[4,5]thiazolo-[3,2-*a*]pyrimidine derivatives. The three-component condensation reactions using 2.5% V_2O_5/FAp as the catalyst and absolute ethanol as solvent at room temperature offered excellent yields for all derivatives in short reaction times (Schemes 1 and 2). We used spectroscopic techniques, TEM, BET, powder-XRD, FT-IR, SEM and EDX analysis to characterise the catalyst material and to confirm all the target molecules fully by NMR and HRMS analysis.

Experimental

V_2O_5/FAp catalyst preparation

We prepared the composites with different wt% of vanadium on fluorapatite (1, 2.5 and 5 wt%) by a co-precipitation adopting the literature reported procedure.[42] 1.5 mmol of trisodium phosphate dodecahydrate ($Na_3PO_4 \cdot 12H_2O$) was suspended in deionised water (25 mL) in a 50 mL of the beaker. Next, 0.5 mmol of sodium fluoride (NaF) was gradually added to that solution under constant stirring for 30 min at room temperature. Then, 2.5 mmol of calcium nitrate tetrahydrate was slowly added to this solution under continuous stirring for a further 15 min. Finally, the calculated volume of 0.5 mmol of 99.9% vanadium oxide was added slowly to the mixture solution, and the stirring continued for 6 h. Subsequently, centrifuged the

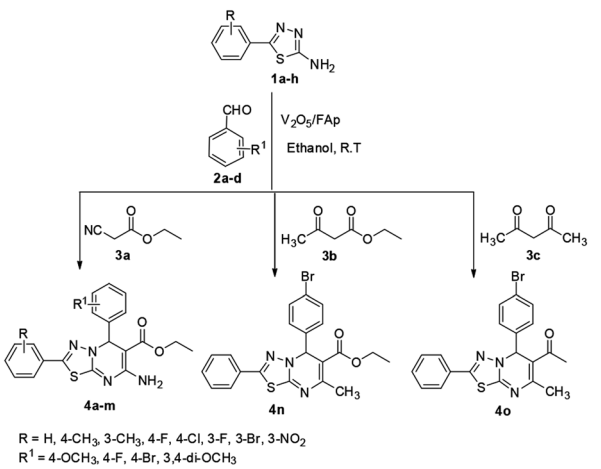

Scheme 1 Multicomponent synthetic route for novel [1,3,4]thiadiazolo[3,2-*a*]pyrimidines.

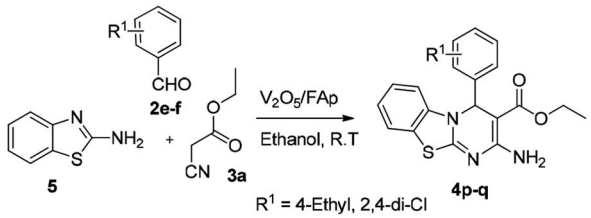

Scheme 2 Multicomponent synthetic route for novel benzo[4,5] thiazolo[3,2-*a*]pyrimidines.

suspension several turns by repetitively rinsing with deionised water. The obtained composite materials were dried in the heating oven at 110 °C for 10 h, followed by calcinated at 350 °C for 4 h under continuous airflow.

General procedure for the synthesis of [1,3,4]thiadiazolo[3,2-*a*]pyrimidine and benzo[4,5]thiazolo[3,2-*a*]pyrimidine derivatives (4a–q)

A mixture of different substituted 1,3,4-thiadiazole-amine (**1a–h**, 1 mmol) or 2-aminobenzathiazole (**5**, 1 mmol), selected benzaldehyde (**2a–f**, 1 mmol) and active methylene compounds (**3a–c**, 1 mmol) together with the heterogeneous catalyst (2.5% V_2O_5/FAp; 30 mg) was added to 5 mL of absolute ethanol solvent in an RB flask. The reaction mixture was kept at R.T for 25 to 30 min under constant stirring. TLC monitored the progress of the reaction. After completion of the reaction, the catalyst was recovered from the reaction mixture by simple filtration, adding excess ethyl acetate. The recovered catalyst material was used for the subsequent cycles. The solvent from the reaction mixture was concentrated by rotatory evaporation under vacuum to harvest the solid product. The product was recrystallised under hot ethanol conditions to achieve the corresponding clean products. Employing different spectroscopic methods (HRMS, FT-IR, ^{1}H and ^{13}C NMR; ESI†), the structures of all synthesised molecules were elucidated.

Results and discussion

Characterisation of the catalyst

Fig. 1 illustrates the SEM, EDX and TEM images of the prepared vanadium oxide loaded fluorapatite (2.5% V_2O_5/FAp) material. The SEM morphology (Fig. 1a) shows the fluorapatite particles arranged in the uniform needle and rod-like shapes and vanadium oxide particles widely in close aggregates on the surface of FAp (Fig. 1c). Fig. 1b exhibits the EDX spectrum, showing the presence of F, P, Ca and V elements in the composite material. The TEM (Fig. 1d) displays the rod-shaped vanadium oxide particles firmly sprouted and masked on the surface of fluorapatite. The average particle size was about 20–30 nm in length and 10–15 nm in diameter.

Fig. 2 illustrates the powder-XRD spectrum of 2.5% V_2O_5/FAp catalyst and the overlying intense peaks with 2θ standards varying between 10° to 80° in the crystalline phases. The intense diffraction signals identified at 2θ values of 25.5°, 29.9°, 32.0°, 34.1°, 40.1°, 46.6°, 48.1°, 50.6°, 53.2° and 55.8° are a good index

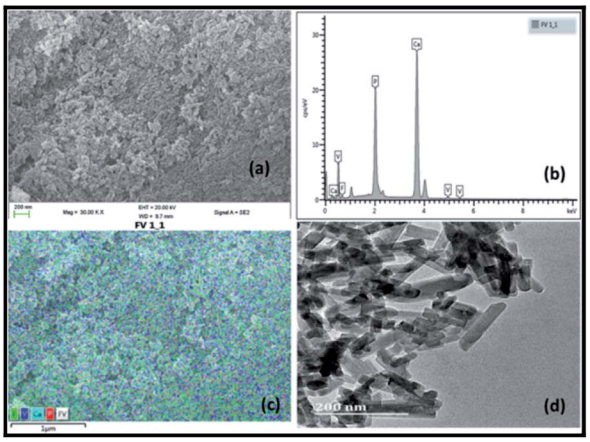

Fig. 1 (a) SEM-micrograph, (b) EDX spectrum, (c) SEM-mapping and (d) TEM-micrograph of 2.5% V_2O_5/FAp catalyst.

of the fluorapatite plans (002), (210), (211), (300), (310), (222), (213), (312), (004) and (322), and were appropriately compatible to the standard pattern of fluorapatite (JCPDS-15-0876). Furthermore, the additional diffraction peaks at 17.5°, 26.5°, 42.2°, 49.4° and 63.0°, and were respectively indexed to the (200), (110), (002), (012) and (711) plans of the V_2O_5 (JCPDS-4-1426).[12] The XRD results confirm the high degree of crystallinity of vanadium oxide loaded on fluorapatite (V_2O_5/FAp).

Fig. 3 shows the Brunauer Emmett Teller (BET) analysis of V_2O_5/FAp composite and nitrogen adsorption–desorption isotherms. The porous properties and BET surface area of the V_2O_5/FAp material were assessed by nitrogen adsorption at 77 K. As-obtained catalyst material can be classified as type-IV isotherm with stepwise desorption and adsorption hysteresis loop and P/P_0 range was 0.76–0.95. The nature of the as-prepared material was a mesoporous material (inset of Fig. 3). The catalyst composite recorded 113.4496 $m^2\ g^{-1}$ of BET surface area, 200.394 Å of pore size and 5692 $cm^3\ g^{-1}$ of the pore volume. The high specific surface areas of V_2O_5/FAp composite might be the reason for the excellent catalytic activity, owing to

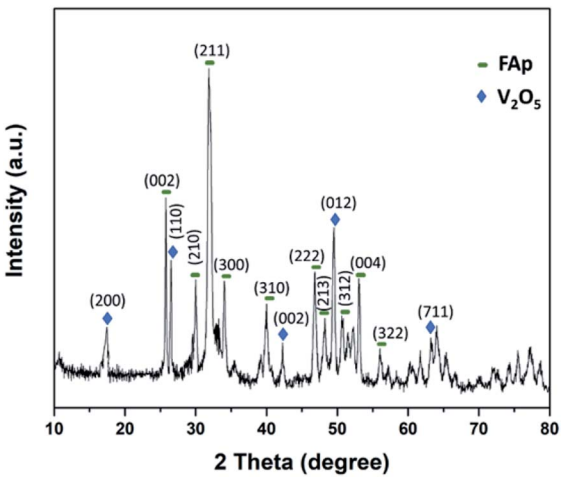

Fig. 2 Powder-XRD spectra of 2.5% V_2O_5/FAp catalyst.

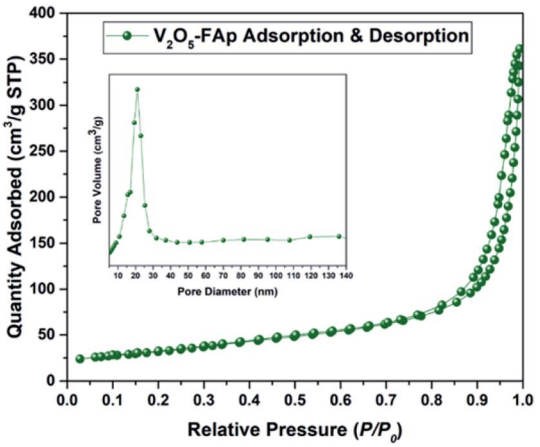

Fig. 3 N_2 adsorption–desorption isotherm spectrum of 2.5% V_2O_5/FAp catalyst.

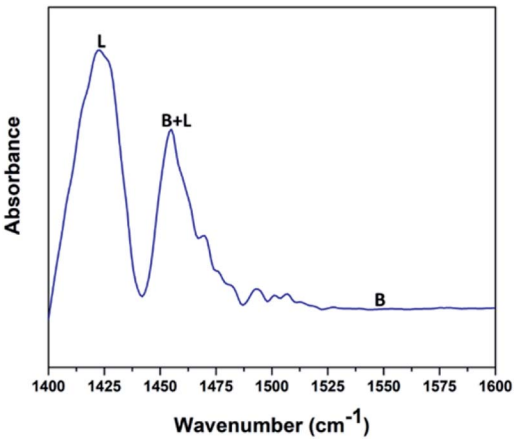

Fig. 5 Pyridine IR spectra of 2.5% V_2O_5/FAp catalyst.

the more active sites over the material surface, facilitating more interactions with substrates.

Fig. 4 illustrates the FT-IR spectra of the V_2O_5/FAp material and the most prominent absorption peaks were at 1417 cm^{-1}, 1020 cm^{-1}, 594 cm^{-1}, and 559 cm^{-1}, from the stretching and bending frequencies of phosphate (PO_4^{3-}) and carbonate (CO_3^{2-}) groups.[42] The stretching vibrational frequency observed at 1417 cm^{-1}, belongs to the carbonate groups (CO_3^{2-}). The most characteristic absorption peak displayed at 1020 cm^{-1} corresponds to the PO_4^{3-} the group of P–O linkages. The other vibrational bands identified at 594 cm^{-1} and 559 cm^{-1} were due to the O–P–O bonds. These results indicate that the calcium phosphate and carbonate ions are on the surface accessible to the reacting substrates.

Fig. 5 shows the pyridine-infrared spectra reflecting the nature of vanadium oxide acidic sites on the FAp surface. The major vibrational peak exhibited at 1422 cm^{-1} represents the Lewis acidic sites on the surface of the V_2O_5/FAp composite. The minor vibrational band at 1454 cm^{-1} indicates both the Brønsted and Lewis acidic sites. No absorption band detected between 1550 and 1600 cm^{-1}, suggests that the no apparent Brønsted acidic sites exist.[43] Therefore, as-obtained material constituted of strong Lewis acidic sites. The catalysed organic reaction is presumably accelerated by the availability of acidic sites on the V_2O_5/FAp material surface.

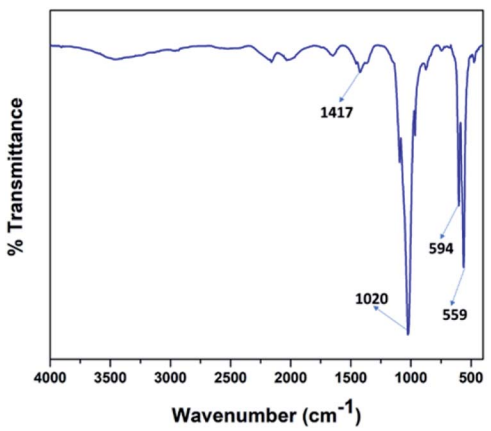

Fig. 4 FT-IR spectra of 2.5% V_2O_5/FAp catalyst.

Catalytic activity

Primarily, we chose 1,3,4-thiadiazole-amine (**1a**), *para*-methoxy benzaldehyde (**2a**) and ethyl cyanoacetate (**3**) as the starting materials for the one-pot reaction (Scheme 1). To identify the appropriate catalyst, we examined the activity of a range of different acidic, basic and metal-oxide catalysts (30 mg per 1 mmol of aldehyde) with ethanol as solvent (Table 1). The reaction in the absence of catalyst gave a trace of the product (**4a**) under both R.T and reflux conditions for about 24 h (Table 1, entry 1). Further, in the presence of different inorganic and organic catalysts such as NaOH, KOH, K_2CO_3, Cs_2CO_3, triethylamine, DABCO and pyridine, gave poor yields of the desired product (**4a**) at room temperature (Table 1, entries 2–8). The reaction examined with various Brønsted acid catalysts also delivered poor yields of the product (Table 1, entries 9–13). Then, the activity with diverse metal oxide catalysts (Table 1, entries 14–17). Among them, vanadium pentoxide (V_2O_5) offered a better yield (62%) of the desired product. Furthermore, the fluorapatite (FAp) also gave a decent product yield (Table 1, entry 18). FAp is amphoteric and can provide both Lewis acidic and basic sites, while $P–O^-$ and F^- are responsible for the Lewis basic sites and Ca^{2+} is responsible for acidic sites.[17] The obtained results reveal that both V_2O_5 and FAp demonstrated promising results as catalysts. Hence, we further investigated the efficacy of the combination of V_2O_5 and FAp, by preparing different wt% (1, 2.5 and 5%) of vanadium oxide loaded on fluorapatite composite (V_2O_5/FAp). Initially, the title reaction was carried out with 1% vanadium oxide on FAp as a catalyst that occurred smoothly offering 88% yield in 30 min (Table 1, entry 19).

By using 2.5% V_2O_5/FAp, the reaction gave a 97% yield, with the reaction time remained unchanged (Table 1, entry 20). Further, with 5% V_2O_5/FAp, unanticipatedly, the yield decreased to 93% (Table 1, entry 21). The variation in the activity of 1, 2.5

Table 1 Effect of catalysts for the synthesis of 1,3,4-thiadiazole-pyrimidine **4a**[a]

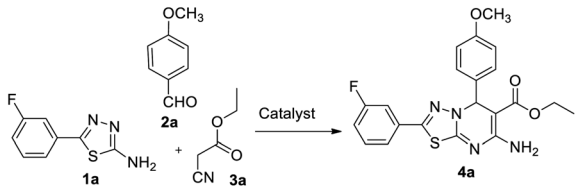

Entry	Catalyst	Reaction conditions	Time (h)	Yield[b] (%)
1	—	R.T/reflux	24	Trace/18
2	NaOH	R.T	12	20
3	KOH	R.T	12	23
4	K_2CO_3	R.T	10.0	19
5	Cs_2CO_3	R.T	8.0	28
6	Et_3N	R.T	8.0	38
7	DABCO	R.T	7.0	24
8	Pyridine	R.T	9.0	17
9	*p*-TSA	R.T	7.0	31
10	HCl	R.T	9.0	29
11	AcOH	R.T	10.0	37
12	H_2SO_4–SiO_2	R.T	5.0	42
13	$HClO_4$–SiO_2	R.T	6.0	39
14	SiO_2	R.T	6.5	41
15	Bi_2O_3	R.T	4.0	52
16	ZnO	R.T	3.5	51
17	V_2O_5	R.T	2.5	62
18	FAp	R.T	1.5	67
19	1% V_2O_5/FAp	R.T	25[c]	88
20	2.5% V_2O_5/FAp	R.T	25[c]	97
21	5% V_2O_5/FAp	R.T	25[c]	93
22	2.5% Bi_2O_3/FAp	R.T	25[c]	79
23	2.5% ZnO_2/FAp	R.T	25[c]	72

[a] Reaction conditions: 1,3,4-thiadiazole-amine (**1a**; 1 mmol), 4-methoxy benzaldehyde (**2a**; 1 mmol), ethyl cyanoacetate (**3a**; 1 mmol) and solvent (5 mL). [b] Isolated yields. [c] Time in min.

and 5 wt% V_2O_5/FAp could be attributed to the available active sites on the catalyst surface, which influence the catalytic efficiency. Generally, the particles are on the surface of the material can act as the Lewis acid centres, and help to activate the organic reactions.[44,45] The 2.5% of V_2O_5/FAp material exhibited superior catalytic activity for the desired product transformation. The efficiency could be due to the even distribution of vanadium oxide nanoparticles on the fluorapatite lattice surface (Fig. 1d). The 1 wt% V_2O_5/FAp material showed lower performance, possibly due to a lesser number of active sites on the catalyst material surface. Though more vanadium is present in 5% V_2O_5/FAp, the inferior activity could be due to higher agglomeration of the vanadia particles on the surface of fluorapatite.[46] With agglomeration, the vanadium oxide particles form clusters, thus lowering the number of available vanadia, hence decreasing the number of available active sites on the catalyst surface to promote the reaction. The properties of the composite of vanadium and fluorapatite are more tunable (stability and acidity) than fluorapatite or vanadia alone.[3,47] The amphoteric nature of fluorapatite and acid sites of V_2O_5 played a crucial role in enhancing the reaction yield. We also examined the efficacy of 2.5% Bi_2O_3/FAp and 2.5% ZnO_2/FAp as catalysts, which respectively gave 79% and 72% yield, but much lower than with V_2O_5/FAp. The better performance could be attributed to the stronger acidic nature of vanadia.

The nature of the solvent varies the solubility of the reactants and catalyst efficiency. Efficacy of different polar-aprotic (DMF, CH_3CN and THF), non-polar (toluene) and polar-protic (H_2O, MeOH and EtOH) solvents were studied (Table 2, entries 2–8). Under solvent-free conditions, the no product formed even after 24 h (Table 2, entry 1). Among all the tested solvents, ethanol proved a superior result. Furthermore, to optimise the amount of 2.5% V_2O_5/FAp, and the reaction was conducted by using the different amounts of catalyst material (10, 20, 30 and 40 mg) (Table 3, entries 1–4). The 10 mg of 2.5% V_2O_5/FAp as catalyst yielded 83% in 50 min reaction time, and 20 mg resulted in the 92% yield in 35 min. The reaction with 30 mg of the catalyst gave a 97% yield in 25 min. No further improvement in the harvest (97%) or reaction time noticed with 40 mg. Therefore, 30 mg of 2.5% V_2O_5/FAp catalyst was taken as the ideal amount and ethanol solvent medium at room temperature as the optimised reaction conditions.

The optimised protocol was used for the synthesis of a series of seventeen [1,3,4]thiadiazolo[3,2-*a*]pyrimidine and benzo[4,5]thiazolo[3,2-*a*]pyrimidine derivatives (**4a–q**) to establish its broader applicability (Schemes 1 and 2). The reactions conducted using different substituted 1,3,4-thiadiazole-amines (**1a–h**) or 2-amino-benzothiazole (**5**) and benzaldehydes (**2a–f**) with varied active methylene compounds, such as ethyl cyanoacetate, ethyl acetoacetate and acetylacetone (**3a–c**) (Table 4) afforded excellent yields (90–97%) of respective functionalized [1,3,4]thiadiazolo[3,2-*a*]pyrimidine and benzo[4,5]thiazolo[3,2-*a*]pyrimidine scaffolds in 25–30 min. Initially, we investigated the scope of 1,3,4-thiadiazole-amine with various aldehydes and ethyl cyanoacetate. We found that various electron-rich and electron-deficient groups substituted on the phenyl ring of the aldehydes were well-tolerated and provided the corresponding products with excellent yields (Table 4, entries **4a–m**). Other active methylene compounds ethyl acetoacetate and acetylacetone, smoothly participated in this reaction and gave impressive yields of 95% and 93%, respectively (Table 4, entries **4n** and **4o**).

Table 2 Screening of solvent effect on reaction time and yield[a]

Entry	Solvent	Time (min)	Yield (%)
1	Solvent-free	1440	—
2	DMF	360	67
3	CH_3CN	120	49
4	Toluene	360	34
5	THF	300	47
6	MeOH	35	83
7	EtOH	25	97
8	Water	90	62

[a] Reaction conditions: 1,3,4-thiadiazole-amine (**1a**; 1 mmol), 4-methoxy benzaldehyde (**2a**; 1 mmol), ethyl cyanoacetate (**3a**; 1 mmol), 2.5% V_2O_5/FAp (30 mg) and solvent (5 mL) at R.T. — no reaction detected.

Table 3 Optimisation of 2.5% V_2O_5/FAp catalyst amount and varying reaction time[a]

Entry	Catalyst (mg)	Time (min)	Yield (%)
1	10	50	83
2	20	35	92
3	30	25	97
4	40	25	97

[a] Reaction conditions1,3,4-thiadiazole-amine (**1a**; 1 mmol), 4-methoxy benzaldehyde (**2a**; 1 mmol), ethyl cyanoacetate (**3a**; 1 mmol) and ethanol (5 mL) at R.T.

Table 4 Synthesis of novel [1,3,4]thiadiazolo[3,2-*a*]pyrimidine and benzo[4,5]thiazolo[3,2-*a*]pyrimidine derivatives by using 30 mg of 2.5% V_2O_5/FAp catalyst[a]

Entry	R	R^1	**3a–c**	Time (min)	Yield[b] (%)
4a	3-F	4-OCH_3	$CNCH_2CO_2Et$	25	97
4b	3-Br	4-OCH_3	$CNCH_2CO_2Et$	28	96
4c	4-CH_3	4-OCH_3	$CNCH_2CO_2Et$	30	93
4d	3-NO_2	4-OCH_3	$CNCH_2CO_2Et$	25	90
4e	3-F	4-F	$CNCH_2CO_2Et$	28	91
4f	3-Br	4-F	$CNCH_2CO_2Et$	30	92
4g	3-CH_3	4-F	$CNCH_2CO_2Et$	25	93
4h	4-Cl	3,4-Di-OCH_3	$CNCH_2CO_2Et$	30	92
4i	H	3,4-Di-OCH_3	$CNCH_2CO_2Et$	28	95
4j	4-F	3,4-Di-OCH_3	$CNCH_2CO_2Et$	25	91
4k	3-F	3,4-Di-OCH_3	$CNCH_2CO_2Et$	30	95
4l	3-Br	3,4-Di-OCH_3	$CNCH_2CO_2Et$	26	91
4m	4-CH_3	3,4-Di-OCH_3	$CNCH_2CO_2Et$	27	92
4n	H	4-Br	$CH_3COCH_2CO_2Et$	28	95
4o	H	4-Br	$CH_2(COCH_3)_2$	30	93
4p	—	4-Et	$CNCH_2CO_2Et$	30	97[c]
4q	—	2,4-Di-Cl	$CNCH_2CO_2Et$	28	96[c]

[a] Reaction conditions: 1,3,4-thiadiazole-amines (**1a–h**) or benzo[*d*] thiazol-2-amine (**5**) (1 mmol), benzaldehydes (**2a–f**) (1 mmol), active methylene compound (**3a–c**) (1 mmol) and ethanol (5 mL) at R.T. [b] Isolated yields. [c] Benzo[*d*]thiazol-2-amine was used as a substrate.

The scope of the reaction was also examined with different groups (F, Cl, Br, NO_2 and CH_3) substituted on the 1,3,4-thiadiazole-amines. In all the cases, the reaction worked well and afforded the desired products in excellent yields (Table 4, entries **4a–d**). Additionally, we examined the scope of amino-azole, the 2-amino-benzothiazole also undergone this reaction smoothly to provide the desired products in significant yields (97% and 96%) (Table 4, entries **4p** and **4q**), at room temperature with ethanol solvent in the presence of 30 mg of the 2.5% V_2O_5/Fap catalyst. Therefore, the present protocol has general applicability and accommodates a diversity of substitution patterns. All the novel derivatives synthesised were fully characterised by various spectroscopic methods, FT-IR, HRMS, ^1H and ^{13}C NMR analysis (ESI†).

Recyclability is one of the vital efficiency parameters of a heterogeneous catalyst. We investigated the reusability of the recovered 2.5% V_2O_5/FAp material. The catalyst was recovered by simple filtration after completion of the reaction from the reaction mixture by washed with ethyl acetate and dried in an oven (110 °C) for 2 h. The dried catalyst was reused, and similar activity was observed up to the fifth run under identical reaction conditions (Fig. 6). The FT-IR and EDX spectra and SEM image of the reused catalyst material after the fifth cycle displayed no significant changes in the morphology and elemental composition as compared to the fresh catalyst (Fig. S1, ESI†). The data supports that there is no erosion of the active material from the support, and the catalyst material proved to be highly robust, preserving its crystalline structure even after repeated use.

The advantage of the present protocol can be acknowledged concisely by comparing the results with the other reported methods with different catalyst materials concerning the reaction time, the yield of the product and reaction conditions. Table 5 demonstrates that the reactions in the current study are considerably faster and give superior returns at room temperature.

The MCRs with V_2O_5/FAp composite as a catalyst displayed greater efficiency compared with the other catalysts reported because of its synergetic effect of the composite. Optimal distribution of the acidic and basic sites on the surface of V_2O_5/FAp composite possibly contributed to its enhanced efficiency, which is evident from the high yields, selectivity and speed of the reaction achieved. Therefore, the composite of vanadium oxide on fluorapatite proves to be a superior catalyst with enormous scope and use in MCRs. Furthermore, the literature survey suggests that there were no reports on the use of V_2O_5/FAp mixed material as a catalyst in any organic synthesis.

Scheme 3 illustrates the proposed mechanism for the creation of 1,3,4-thiadiazole-pyrimidine *via* a three-component one-pot condensation reaction. The reaction probably occurs on the surface of V_2O_5/FAp, as it can provide necessary Lewis acidic and basic sites to catalyse the reaction. The carbonyl (C=O) group of aldehydes (**2a**) adsorbed on the acidic sites of vanadia on the surface of the catalyst, get activated leading to the Knoevenagel condensation with active methylene compound (**3a**), furnishing a key condensation intermediate (**I**). There can be two possible mechanistic pathways. Meanwhile, the Brønsted and Lewis basic sites of catalyst (FAp) coordinate with the 1,3,4-thiadiazole-amine (**1a**) and facilitate the

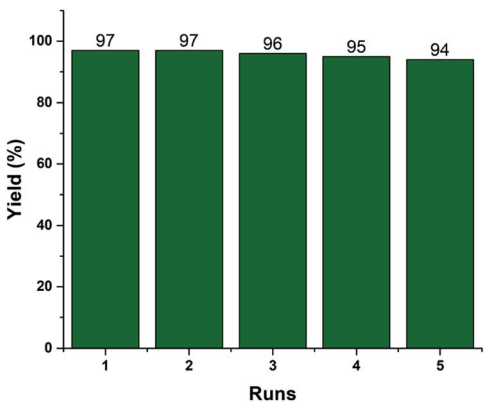

Fig. 6 Recyclability of 2.5% V_2O_5/FAp catalyst.

Table 5 Comparison of the 2.5% V_2O_5/FAp catalyst with other reported catalysts for the synthesis of 1,3,4-thiadiazole- and benzothiazole-pyrimidines

S. no.	Catalyst	Reaction conditions	Time (min)	Yield (%)
1	Catalyst-free[a]	Microwave/65 °C/acetic acid	40	85 (ref. 36)
2	NaOH[a]	Ultrasonic/80 °C/ethanol	60	89 (ref. 37)
3	PEG-400[a]	80 °C/PEG-400	360	80 (ref. 38)
4	P_2O_5[a]	100 °C/HCOOH	720	93 (ref. 25)
5	*p*-TSA[a]	Microwave/100 °C/water	5	96 (ref. 48)
5	Fe_3O_4@nano-cellulose/ Cu(II)[b]	80 °C/solvent-free	30	97 (ref. 26)
6	Nano-kaolin/Ti^{4+}/Fe_3O_4[b]	100 °C/solvent-free	90	95 (ref. 39)
7	Nano-cellulose/BF_3/Fe_3O_4[b]	100 °C/solvent-free	45	98 (ref. 40)
8	Nano-Fe_3O_4@SiO_2–$TiCl_3$[b]	100 °C/solvent-free	45	90 (ref. 41)
9	2.5% V_2O_5/FAp	RT/ethanol	<30	97 (This work)

[a] Synthesised 1,3,4-thiadiazolo[3,2-*a*]pyrimidines. [b] Synthesised benzo[4,5]thiazolo[3,2-*a*]pyrimidines.

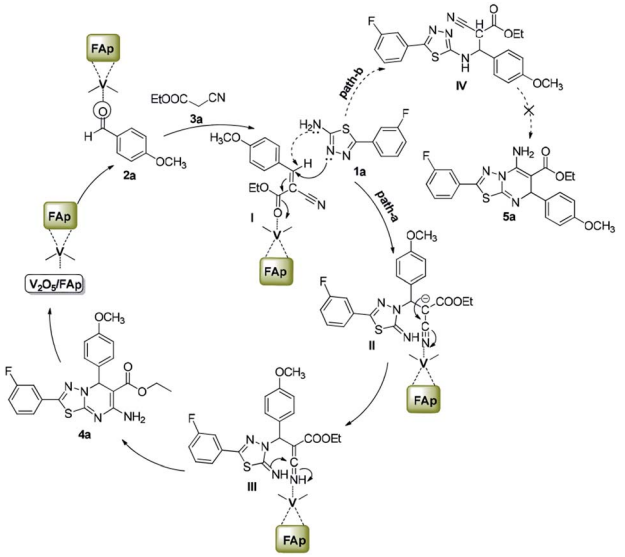

Scheme 3 The probable reaction mechanism for the formation of [1,3,4]thiadiazolo[3,2-*a*]pyrimidines.

rearrangement of electrons, which promote a Michael type addition with condensed intermediate (**I**) generating intermediate (**II**) in the path-A. The transient intermediate (**II**), finally undergoes an intramolecular cyclisation, followed the ring closer to give the target 1,3,4-thiadiazole-pyrimidine derivative (**4a**).

Alternatively, in path-B, 1,3,4-thiadiazole-amine (**1a**) may also react with the intermediate (**I**) *via* 1,3-addition reaction to generate intermediate **IV**, which constitutes a minor pathway. However, we did not observe product **5a**. These reactions preferably go through a nucleophile attack, *via* a regioselective β-carbon of intermediate (**I**).[48] The role of V_2O_5/FAp probably would be Lewis acidic characteristic for the activation of the nitrile to transform into an amine. Therefore, amphoteric properties of V_2O_5/FAp composite with the synergic effect and a high specific surface area containing V_2O_5/FAp enhance the number of active catalytic sites, which proves it as a highly efficient catalyst in these value-added one-pot reactions.

Conclusions

Using V_2O_5/FAp as a catalyst, we reported a highly efficient one-pot protocol for the synthesis of seventeen novel [1,3,4]thiadiazolo[3,2-*a*]pyrimidine and benzo[4,5]thiazolo[3,2-*a*]pyrimidine analogues. The synergy between the strong acidic properties of vanadia and the amphoteric nature of 2.5% V_2O_5/FAp composite exhibited superior catalytic activity in ethanol medium at R.T. offering excellent yield (90–97%) of the target products in 25–30 min. TEM, BET, SEM, XRD, EDX and FT-IR analysis were used to characterise the prepared catalyst materials. In comparison with other reported catalysts, the V_2O_5/FAp promoted reaction offers high yields of products at room temperature in shorter reaction time. Other benefits of the proposed protocol are simple separation and recyclability catalyst, green solvent and no need for column chromatography. Furthermore, this method delivers an excellent atom economy (97%) and carbon efficiency (100%) with remarkable economic and eco-friendly returns.

Conflicts of interest

There are no conflicts to declare.

Acknowledgements

The authors are thanks to the University of KwaZulu-Natal, Durban, South Africa for financial support and research facilities.

References

1 G. J. Hutchings, *J. Mater. Chem.*, 2009, **19**, 1222–1235.
2 A. Fihri, C. Len and R. S. Varma, *Coord. Chem. Rev.*, 2017, **347**, 48–76.

3 W. Wang, W. Du, Y. Zhang, A. Wang and L. Zhang, *React. Kinet., Mech. Catal.*, 2018, **125**, 965–981.
4 P. Comodi, Y. Liu, P. F. Zanazzi and M. Montagnoli, *Phys. Chem. Miner.*, 2001, **28**, 219–224.
5 S. Sebti, R. Tahir, R. Nazih, A. Saber and S. Boulaajaj, *Appl. Catal., A*, 2002, **228**, 155–159.
6 H. E. Mason, F. M. McCubbin, A. Smirnov and B. L. Phillips, *Am. Mineral.*, 2009, **94**, 507–516.
7 M. Zahouily, Y. Abrouki, B. Bahlaouan, A. Rayadh and S. Sebti, *Catal. Commun.*, 2003, **4**, 521–524.
8 K. Mori, T. Hara, T. Mizugaki, K. Ebitani and K. Kaneda, *J. Am. Chem. Soc.*, 2003, **125**, 11460–11461.
9 T. Hara, S. Kanai, K. Mori, T. Mizugaki, K. Ebitani, K. Jitsukawa and K. Kaneda, *J. Org. Chem.*, 2006, **71**, 7455–7462.
10 K. Pajor, L. Pajchel and J. Kolmas, *Materials*, 2019, **12**, 2683.
11 S. V. H. S. Bhaskaruni, K. K. Gangu, S. Maddila and S. B. Jonnalagadda, *Chem. Rec.*, 2019, **19**, 1793–1812.
12 S. Maddila, S. N. Maddila, S. B. Jonnalagadda and P. Lavanya, *J. Heterocycl. Chem.*, 2016, **53**, 658–664.
13 S. V. H. S. Bhaskaruni, S. Maddila, W. E. van Zyl and S. B. Jonnalagadda, *Catal. Today*, 2018, **309**, 276–281.
14 V. D. B. C. Dasireddy, S. Singh and H. B. Friedrich, *Appl. Catal., A*, 2013, **456**, 105–117.
15 J. Sun, X. Li, Q. Zhao, J. Ke and D. Zhang, *J. Phys. Chem. C*, 2014, **118**, 10113–10121.
16 X. Liu, J. Zeng, H. Yang, K. Zhou and D. Pan, *RSC Adv.*, 2018, **8**, 4014–4031.
17 K. K. Gangu, S. Maddila, S. N. Maddila and S. B. Jonnalagadda, *Molecules*, 2016, **21**, 1281.
18 S. N. Maddila, S. Maddila, N. Kerru, S. V. H. S. Bhaskaruni and S. B. Jonnalagadda, *ChemistrySelect*, 2020, **5**, 1786–1791.
19 N. Kerru, L. Gummidi, S. N. Maddila, S. V. H. S. Bhaskaruni and S. B. Jonnalagadda, *Appl. Organomet. Chem.*, 2020, **34**, e5590.
20 N. Kerru, L. Gummidi, K. K. Gangu, S. Maddila and S. B. Jonnalagadda, *ChemistrySelect*, 2020, **5**, 4104–4110.
21 H. Sheibani and F. Hassani, *J. Heterocycl. Chem.*, 2011, **48**, 915–920.
22 E. A. El-Rady, *J. Heterocycl. Chem.*, 2014, **51**, 869–875.
23 N. Seyyedi, F. Shirini, M. Safarpoor, N. Langarudi and S. Jashnani, *J. Iran. Chem. Soc.*, 2017, **14**, 1859–1867.
24 W. M. Basyouni, S. Y. Abbas, N. M. Abdelazeem, K. A. M. El-Bayouki and M. Y. El-Kady, *Synth. Commun.*, 2019, **49**, 3112–3120.
25 H. R. Dong, Z. L. Gao, R. S. Li, Y. M. Hu, H. S. Dong and Z. X. Xie, *RSC Adv.*, 2014, **4**, 55827–55831.
26 N. Safajoo, B. B. F. Mirjalili and A. Bamoniri, *RSC Adv.*, 2019, **9**, 1278–1283.
27 F. A. Ragab, H. I. Heiba, M. G. El-Gazzar, S. M. Abou-Seri, W. A. El-Sabbagh and R. M. El-Hazek, *RSC Med. Chem.*, 2016, **7**, 2309–2327.
28 D. Cai, Z. H. Zhang, Y. Chen, X. J. Yan, S. T. Zhang, L. J. Zou, L. H. Meng, F. Li and B. J. Fu, *Med. Chem. Res.*, 2016, **25**, 292–302.
29 S. F. Mohamed, E. M. Flefel, A. G. Amr and E. Shafy, *Eur. J. Med. Chem.*, 2010, **45**, 1494–1501.
30 A. D. Borthwick, D. E. Davies, P. F. Ertl, A. M. Exall, T. M. Haley, G. J. Hart, D. L. Jackson, N. R. Parry, A. Patikis, N. Trivedi, G. G. Weingarten and J. M. Woolven, *J. Med. Chem.*, 2003, **46**, 4428–4449.
31 E. Flefel, M. Salama, M. El-Shahat, M. El-Hashash and A. El-Farargy, *Phosphorus, Sulfur Silicon Relat. Elem.*, 2007, **182**, 1739–1756.
32 B. Pan, R. Huang, L. Zheng, C. Chen, S. Han, D. Qu, M. Zhu and P. Wei, *Eur. J. Med. Chem.*, 2011, **46**, 819–824.
33 M. T. Gabr, N. S. El-Gohary, E. R. El-Bendary and M. M. El-Kerdawy, *Eur. J. Med. Chem.*, 2014, **85**, 576–592.
34 N. S. El-Gohary and M. I. Shaaban, *Arch. Pharm. Chem. Life Sci.*, 2015, **348**, 283–297.
35 M. E. Azab, S. S. Abdel-Wahab, N. F. Mahmoud and G. A. Elsayed, *J. Heterocycl. Chem.*, 2018, **55**, 2349–2359.
36 B. Zhao, Y. Xu, Q. G. Deng, Z. Liu, L. Y. Wang and Y. Gao, *Tetrahedron Lett.*, 2014, **55**, 4521–4524.
37 S. V. Tiwari, J. A. Seijas, M. P. Vazquez-Tato, A. P. Sarkate, D. K. Lokwani and A. P. G. Nikalje, *Molecules*, 2016, **21**, 894.
38 S. Kasaboina, R. Bollu, P. M. Gomedhika, V. Ramineni, L. Nagarapu, N. Dumala, P. Grover and J. B. Nanubolu, *Tetrahedron Lett.*, 2018, **59**, 3015–3019.
39 B. B. F. Mirjalili and R. Soltani, *RSC Adv.*, 2019, **9**, 18720–18727.
40 B. B. F. Mirjalili and F. Aref, *Res. Chem. Intermed.*, 2018, **44**, 4519–4531.
41 S. A. Fazeli-Attar and B. B. F. Mirjalili, *Res. Chem. Intermed.*, 2018, **44**, 6419–6430.
42 K. K. Gangu, S. Maddila, S. N. Maddila and S. B. Jonnalagadda, *RSC Adv.*, 2016, **6**, 58226–58235.
43 J. Sun, K. Zhu, F. Gao, C. Wang, J. Liu, C. H. F. Peden and Y. Wang, *J. Am. Chem. Soc.*, 2011, **133**, 11096–11099.
44 F. M. Moghaddam and H. Saeidian, *Mater. Sci. Eng., B*, 2007, **139**, 265–269.
45 S. Farhadi and M. Zaidi, *J. Mol. Catal. A: Chem.*, 2009, **299**, 18–25.
46 N. Kerru, S. V. H. S. Bhaskaruni, L. Gummidi, S. N. Maddila, S. Rana, P. Singh and S. B. Jonnalagadda, *Appl. Organomet. Chem.*, 2019, **33**, e4722.
47 S. Sumathi and B. Gopal, *React. Kinet., Mech. Catal.*, 2016, **117**, 77–86.
48 P. Wadhwa, T. Kaur, N. Singh, U. P. Singh and A. Sharma, *Asian J. Org. Chem.*, 2016, **5**, 120–126.

